Engineered Science
DOI: https://dx.doi.org/10.30919/es1251

Prediction of Ultimate Strain in Anchored Carbon Fibre-Reinforced Polymer (CFRP) Laminates using Machine Learning

Sabreen Dar Amer,[1] Maha Assad,[1] Rami A. Hawileh,[1] Ghada Karaki,[2,*] Hussam Safieh[1] and Jamal Abdalla[1]

Abstract

Anchoring carbon fibre-reinforced polymer (CFRP) laminates to concrete using CFRP spike anchors effectively mitigates the unfavorable debonding failure mode in strengthened concrete beams. However, the strain and strength enhancement resulting from anchoring CFRP laminates have not been thoroughly quantified in the literature and existing practice codes. This study investigates the prediction of ultimate strain in anchored CFRP laminates, which is critical for assessing the flexural strength of strengthened concrete beams. Statistical regression analysis and machine learning models are employed to develop a predictive equation for the ultimate strain in CFRP laminates due to anchorage, using data from prior flexural tests on concrete prisms. The study examines various parameters, including CFRP sheet width, anchor design details (such as diameter and embedment depth), number of CFRP layers and anchor-to-sheet material ratio. Linear regression models, Support Vector Regression and Decision Trees were tested and compared for their accuracy in predicting the ultimate strain in CFRP laminates. The linear regression model, with highest performance indicators, was selected. Additionally, the study provides derived predictive equations, offering a practical implication for design optimization. Finally, sets of design charts were proposed to achieve specific values of ultimate strain in CFRP-strengthened and anchored concrete beams.

Keywords: FRP anchors; Flexural strengthening; Regression; Machine learning; Design optimization.
Received: 28 May 2024; Revised: 01 August 2024; Accepted: 21 August 2024.
Article type: Research article.

1. Introduction

Fiber-reinforced polymers (FRP) are widely adopted in strengthening and rehabilitation of existing reinforced concrete (RC) structures.[1–3] They offer a wide range of positive characteristics, including ease of installation, high strength, low weight, and corrosion resistance, especially carbon fiber-reinforced polymers (CFRP),[4,5] which exhibit a linear elastic behavior until rupture. The flexural strengthening of RC beams using CFRP sheets is widely implemented in structural engineering and is extensively studied in the literature.[6–12] CFRP sheets usually adhere to the tension side of the beam using epoxy adhesives, which form the CFRP laminates. The main drawback of this strengthening system is the brittle failure of strengthened beams when CFRP laminates detach from the concrete substrate, which is a well-documented debonding phenomenon. This failure mode occurs at a much lower strain than the ultimate rupture strain. Thus, the strength of CFRP is not fully utilized. This is why standard design guidelines specify the maximum strain in the FRP to be limited by the debonding strain, where each design code has a standard formula for its calculation. A possible remedy to the debonding problem is to anchor the CFRP laminates to the beam. Different anchorage techniques were proposed in the literature, *e.g.* mechanical anchorage[13] or CFRP U-wraps.[14,15] However, there are limitations related to such anchorage systems, including the corrosion of mechanical anchors and the hurdles associated with the attachment of the U-wraps. Anchoring CFRP laminates using CFRP spike anchors has been proven to be a highly effective technique to mitigate debonding failure of the laminates.[16–20] The CFRP anchor comprises a bundled fibre sheet soaked in epoxy resin. Three components form the FRP anchor. The dowel is inserted in a predrilled hole in the concrete member, the fan is the portion splayed on the FRP sheet with epoxy, and the key portion is where the fan transitions into the dowel.

Several previous studies investigated the effect of CFRP anchors on the debonding mechanism.[21–24] Most studies examined the bond strength of the anchored laminates through pull-off shear tests, where laminate that is adhered and

[1] *Civil Engineering Department, American University of Sharjah, Sharjah 26666, United Arab Emirates.*
[2] *School of Engineering, University of the West of England, Bristol BS16 1QY, United Kingdom.*
**Email:* Ghada.Karaki@uwe.ac.uk (G. Karaki)

anchored to the concrete surface is pulled using a tensile force until failure of the anchored joint occurs. The potential failure modes in this test include anchor rupture, anchor pullout, sheet/plate debonding, or a combination of anchor's failure with sheet/plate debonding. In general, it was found that the strain at which the sheet detaches from concrete in anchored FRP-to-concrete joints increases with proper anchorage. The degree of strain utilization depends on the anchor and sheet parameters, including but not limited to the number and location of anchors, number of sheets, and design parameters of the anchor (embedment depth, fan length, fanning angle, and dowel insertion angle). Although such tests give good insights into the effectiveness of the anchor's design, they require careful consideration regarding the specimen's alignment, fixture of the concrete block, and adequacy of the grip between the pulling force and the FRP sheet. Jimenez and Maria[25] analyzed the effect of multiple parameters of the CFRP anchors with varying dowel angles. They utilized finite element analysis and created a three-dimensional model that can predict the strength of the direct shear joint between the anchored CFRP joint and concrete. Their model results showed that the joint strength is influenced by the unbonded length (length of the CFRP ply beyond the anchor) and the dowel's angle. Zhou *et al*.[26] presented an analytical study that accounted for the bond behavior of CFRP-concrete anchored joints with end-anchors. The authors used the proposed analytical solution to perform a parametric study to investigate the effect of mechanical properties of end-anchors on the overall bond behavior of the joint. The study concluded that the anchor's yield strength should be slightly less than the CFRP rupture strength to allow for the development of a ductile deformation.

Tests conducted on FRP-to-concrete anchored joints that represent the actual behavior of the joint in a flexural system include testing concrete prisms or RC beams, strengthened and anchored with CFRP laminates and CFRP anchors.[27–31] In these tests, the beam is subjected to a three-point or four-point bending, and the beams' behavior is monitored by measuring the midspan deflection and the strain in the FRP laminate during the test. Sun conducted 38 three-point bending tests on strengthened and anchored concrete prisms. The author varied the width of the CFRP strip, the anchor's area to the sheet's area ratio (AMR), hole diameter, anchor's embedment depth, and concrete compressive strength. The results show that the optimum fanning angle of the anchor should be 45, the embedment depth should not be less than 102 mm, and the AMR value should be between 2.2 and 4.85.[20] Pudleiner also tested 12 small-scale prisms under a three-point bending test.[32] The author indicated that anchors provide additional strength gain after full debonding of the CFRP occurs. Alotaibi *et al*.[33] developed a database based on Sun and Pudleiner's studies[20,32], aiming to provide simple detailing-based design recommendations for CFRP anchors. The database consisted of 51 bending tests. The provided anchor design recommendations were based on derivations from the results and conclusions of the studied tests in terms of failure modes, ultimate strain, and maximum load capacity. The authors recommended that the AMR ratio should not be less than 2.0. They also provided equations for the suitable anchor fan and anchor hole details.

Few attempts were made to predict the ultimate strain in the anchored FRP laminate. Al Sammari and Brena used the data from previously conducted single shear tests on FRP-to-concrete anchored joints to perform a regression analysis to predict the ultimate strain in the CFRP laminates.[34] They proposed an anchorage efficiency factor multiplied by the debonding equation in ACI-440.2R-19.[35] This factor depends on the number of anchors, spacing between anchors, anchor diameter, fan diameter, and CFRP sheet's width. The authors compared the proposed efficiency factor with the values obtained from previous experimental studies. The average ratio between proposed and actual values was 0.93, with a standard deviation of 0.12. However, this factor is developed based on shear tests and needs to be verified with flexural tests on FRP-strengthened and anchored beams.

Zaki *et al*.[36] tested three full-scale T-beams and three rectangular beams under a four-point bending test. The beams contained one control specimen of each type, and the rest were strengthened with CFRP sheets and anchored along the shear span using either U-wraps or FRP anchors. The authors proposed a multiplier coefficient for the ACI440.2R-19 equation of debonding strain.[35] This multiplier accounted for the development in strain due to the sheet anchorage and was determined by dividing the load at experimental failure by the predicted load at FRP debonding strain. The highest multiplier value corresponded to the T-beam having 16 mm diameter anchors, which was 1.66. The rectangular beam with 19 mm anchors had the lowest multiplier value of 1.11. Nevertheless, these factors were developed using a small number of experiments and did not depend on the sheet or anchors' details. As a result, the factors may not be generalized for other designs. In another recent experimental investigation performed by Rasheed *et al*.[37] researchers addressed the effectiveness of the CFRP spike anchors in controlling the debonding failure of the CFRP sheets by testing five strengthened RC T-beams, anchored with various number of CFRP anchors along the shear span under four-point bending. The study revealed that using six anchors along the shear span prevented the debonding of the CFRP sheet. The authors also indicated that anchors could be optimized to obtain a specific target debonding strain higher than the debonding strain, depending on the design objective and desired level of strength utilization. However, only one specimen was tested per anchors' configuration. Therefore, the authors highlighted the need for more research to confirm the applicability of the results.

Thus far, and considering the abovementioned review, there is a need to quantify the additional strength resulting from anchoring CFRP sheets attached to concrete beams using CFRP spike anchors. This study uses data from previously

published flexural tests on concrete beams to utilize statistical regression analysis and machine learning models to predict the ultimate strain in the anchored CFRP sheets. The study aims to develop an equation for the prediction of strain that considers the anchors' design details. Predicting the ultimate strain would accurately assess the flexural strength of strengthened and anchored beams. Through the solution of the ultimate strain equation, this paper provides recommendations for a combination of the optimum values of CFRP sheet width, anchor's diameter, AMR, and anchor's embedment depth.

2. Data analysis

This section presents the datasets used in the analysis, reliability measurements of the collected database, and statistical characteristics of the data, including variability and correlation. Moreover, the analysis methodology using statistical modeling and machine learning is explained.

2.1 Methodology

The analysis framework is illustrated in Fig. 1. First, data collection was performed from flexural tests of strengthened and anchored concrete prisms. Following data collection, a reliability analysis is conducted to assess the consistency of the data. This involves calculating Cronbach's Alpha, a measure of internal consistency, indicating how closely related a set of items are as a group. The core of the analysis involves developing regression and ML-based models to understand the relationships between input variables and the target variable, which in this case is the ultimate strain (ε_u). The regression-based methods used include linear regression, which is fundamental for determining linear relationships. On the ML-based side, Support Vector Machines (Linear SVM) and Decision Trees are employed for the regression. The models are then validated to ensure their predictive power and accuracy. This is typically done through statistical measures like the coefficient of determination (R^2), which indicates the proportion of the variance for the dependent variable that's predictable from the independent variables, and the Mean Squared Error (MSE), which measures the average of the squares of the errors, that is, the average squared difference between the estimated values and the actual value. Based on the validation metrics, the most accurate regression model is chosen to propose a prediction equation for the ultimate strain (ε_u). This step is crucial to ensure that the model fits the data well and generalizes to new, unseen data. The chosen model's accuracy is further validated by calculating the discrepancy between the model's predictions and the actual observed values. Finally, the developed model proposes a set of design values for CFRP sheets and anchors' parameters. These values are not merely theoretical but are derived from empirical data and are meant to serve as practical recommendations for designing and reinforcing concrete beams with CFRP anchors.

2.2 Datasets

The database used in this study is presented in Table 1, which consists of data collected from Sun *et al.*[27], Pudleiner *et al.*[32] and Alshami *et al.*[31] All specimens were concrete prisms. In [27], the prism dimensions were in accordance with ASTM C293.17.[38] Specifically, the specimens were 152 mm wide by 152 mm by 610 mm long. The specimens used in Pudleiner *et al.*[32] had a width and depth of 305 mm, respectively, and a length of 1727 mm. The prisms in Alshami *et al.*[31] had a length of 750 mm, a width and a thickness of 150 mm, respectively. The properties of CFRP sheets and laminates (sheets + epoxy) are listed in Table 1. The input parameters included width of the CFRP sheet (w) anchor-to-sheet material ratio (AMR), dowel diameter of the CFRP anchor (d_a), dowel's embedment depth (h_e), concrete compressive strength (f'_c), and number of CFRP sheets (n). Whereas the output parameter is the ultimate strain in the CFRP sheet (ε_u). Fig. 2 illustrates the components of the FRP anchor. AMR can be calculated as the ratio between the cross-sectional area of the anchors to the cross-sectional area of the fiber sheet:

$$AMR = \frac{A_a}{A_f} = \frac{N_a \frac{\pi}{4} d_a^2}{n w t_f} \quad (1)$$

where, A_a is the cross-sectional area of the FRP anchor (mm^2); A_f cross-sectional area of the FRP laminate (mm^2); $N_a$is the number of anchors; d_a is the diameter of the anchor dowel (mm); n is the number of FRP plies; w is the width of the FRP strip (mm); and t_f is the thickness of the FRP strip (mm).

Figure 3 illustrates the variation of the ultimate strain with the given data of each parameter. The database illustrated in Fig. 3 and Table 2 for strengthened concrete prisms with CFRP anchors provides a variety of input parameters critical for the ultimate strain (ε_u) enhancement due to CFRP sheet's anchorage. The width of CFRP sheets varies significantly across the studies, ranging from as narrow as 76.2 mm to as wide as 254.0 mm. A wider sheet potentially offers more reinforcement area but also introduces considerations regarding the bond to the concrete surface and the stress transfer efficiency. AMR values in the database range from 1.1 to 2.8. This ratio indicates the relative amount of material used in the anchor compared to the CFRP sheet. Higher ratios suggest a stronger emphasis on the anchoring system, potentially to enhance the bond or to prevent premature failure modes such as debonding or pullout. The diameters of the CFRP dowel anchors included in the studies vary from 8.00 mm to 41.40 mm. The diameter of the anchor dowel plays a crucial role in the anchorage system, affecting both the mechanical interlock with the concrete and the stress distribution around the anchor. The embedment depth of the dowels ranges from 50.00 mm to 152.4 mm. This parameter is critical for ensuring adequate anchorage strength. Many entries have an embedment depth of 101.6 mm; other notable depths are 75.00 mm and 152.4 mm. The concrete

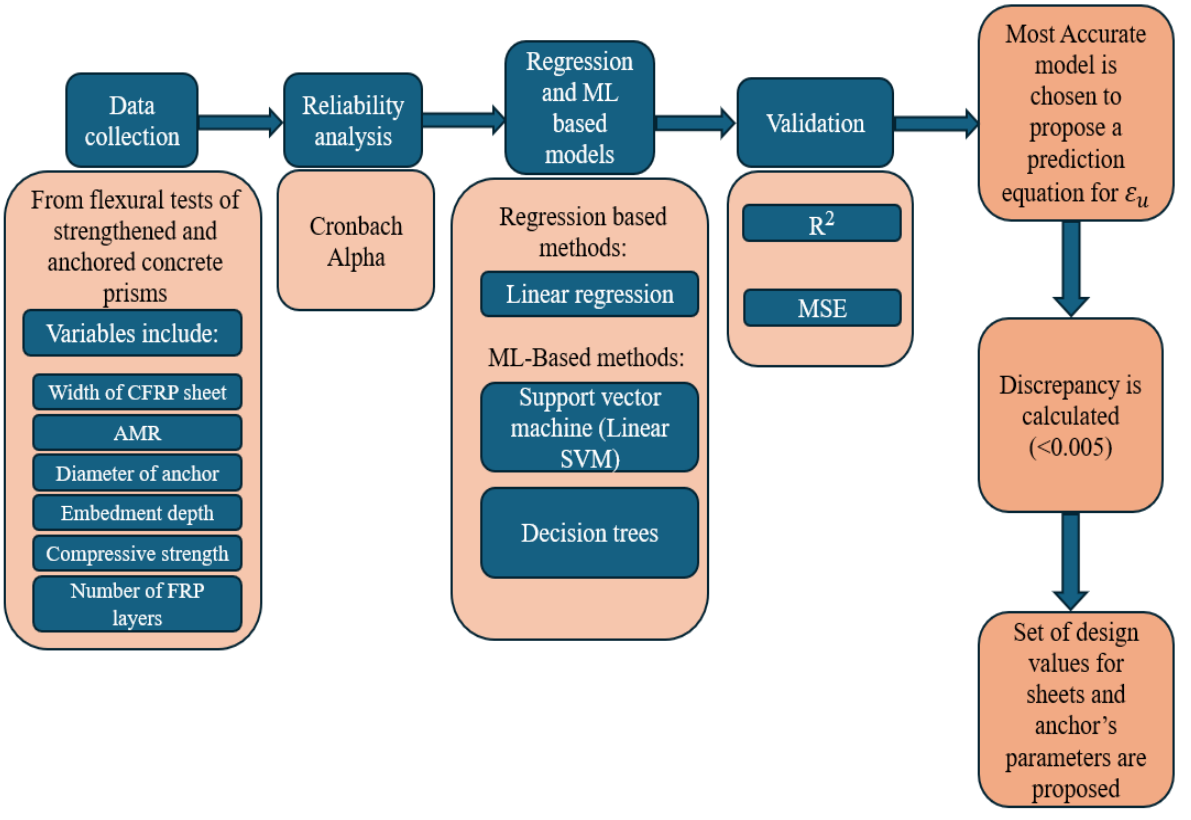

Fig. 1 Flowchart of the study's framework.

Table 1. Properties of CFRP.

Reference	Material	Tensile strength (MPa)	Tensile modulus (GPa)	Ultimate elongation (%)	Thickness (mm)
Pudleiner *et al.*[32], Sun[20]	CFRP dry fibers	3826	230.3	1.7%	-
	CFRP laminate	986	96.84	1.0%	0.508
Alshami *et al.*[31]	CFRP dry fibers	4900	252	2%	0.164
	CFRP laminate	1637	83.85	1.6%	0.5

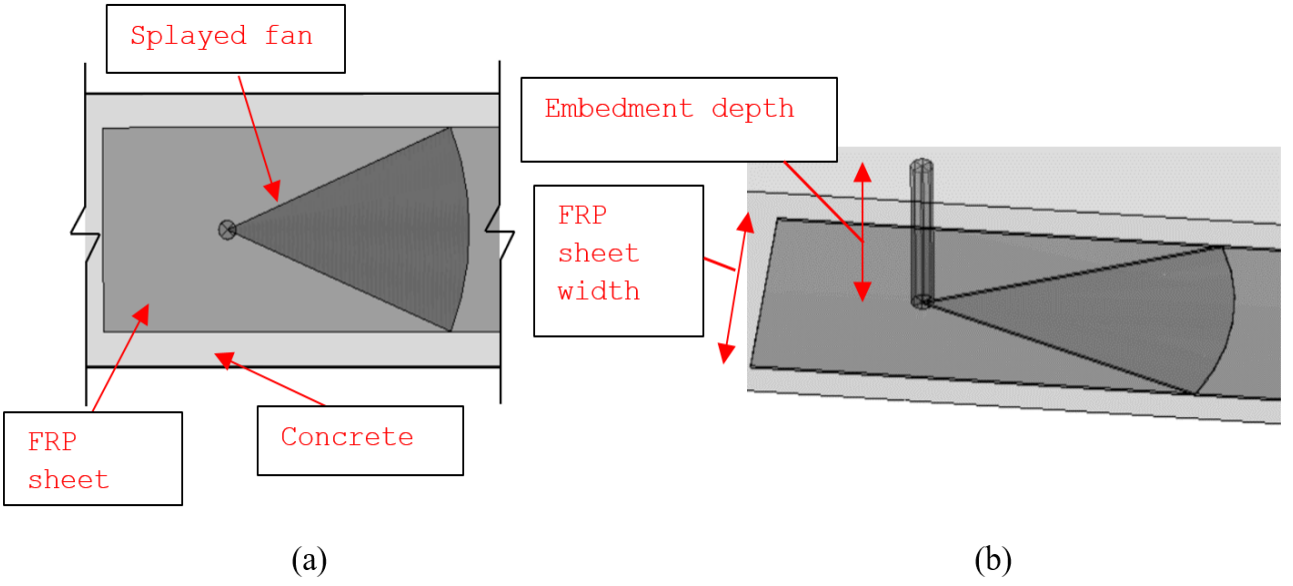

Fig. 2 Schematic of CFRP spike anchor in FRP-strengthened concrete. (a) Bottom view of anchored sheet. (b) 3-D view inside strengthened and anchored concrete.

Table 2. Database of strengthened concrete prisms with CFRP anchors.

Reference	w (mm)	AMR	d_a (mm)	h_e (mm)	f'_c (MPa)	n	ε_u (mm/mm)
Pudleiner *et al.*[32]	127.0	1.7	15.88	101.6	60.70	1	0.0129
	203.2	2	22.23	101.6	62.08	1	0.0101
	254.0	1.7	15.88	101.6	62.08	1	0.0107
	127.0	2.8	25.40	101.6	68.29	2	0.0093
	254.0	2	22.23	101.6	68.29	1	0.0141
	254.0	2.8	25.40	152.4	68.29	2	0.0112
	127.0	2.8	25.40	152.4	35.18	2	0.0107
	254.0	2.8	41.40	152.4	35.18	2	0.0127
	254.0	2	31.75	152.4	24.83	2	0.0128
Sun[20]	127.0	2	19.05	101.6	79.32	1	0.0135
	127.0	1.4	15.88	101.6	79.32	1	0.0132
	127.0	1.1	15.88	101.6	79.32	1	0.0136
	127.0	1.1	11.11	101.6	37.25	1	0.0119
	127.0	1.1	15.88	101.6	37.25	1	0.0134
	127.0	2	19.05	101.6	79.32	1	0.0126
	127.0	1.4	16.00	101.6	79.32	1	0.0134
	127.0	2	19.05	101.6	79.32	1	0.0158
	76.2	1.4	15.88	101.6	37.25	1	0.0148
	76.2	1.1	15.88	101.6	37.25	1	0.0145
Alshami *et al.*[31]	100.0	1.6	10.00	75.00	50.00	1	0.007409
	100.0	1.25	8.00	75.00	50.00	1	0.005281
	100.0	2.1	12.00	75.00	50.00	1	0.008244
	100.0	1.6	10.00	50.00	50.00	1	0.005801
	100.0	1.6	10.00	100.0	50.00	1	0.008896
	100.0	1.6	10.00	125.0	50.00	1	0.010642
	100.0	1.6	10.00	75.00	50.00	1	0.009313

compressive strength covered in the database spans from 24.83 MPa to 79.32 MPa. However, there is a noticeable concentration of values around 50.00 MPa and 68.29 MPa. This suggests that a significant portion of the studies focused on medium to high-strength concrete. Finally, most cases use a single CFRP sheet, with fewer instances of using two sheets. This pattern suggests that single-sheet reinforcement is the most common approach, likely due to its simplicity, cost-effectiveness, and adequacy for many strengthening objectives.

Figure 4 shows the frequency of each input variable. The histograms depicted in the figure collectively suggest an imbalanced data distribution across several input categories. Such an imbalance can pose significant challenges for machine learning models. Specifically, when specific categories are overrepresented and others are underrepresented, models may become biased towards predictions that work well for the majority class but fail to predict outcomes for the minority classes accurately. This is because the model has fewer examples to learn from for these underrepresented categories, leading to a lack of generalizability when encountering new or varied data points. Consequently, this can result in poor model performance, particularly in practical applications where the input data may not match the distribution of the training dataset. Attempts were made to include more data from published studies. However, data from strengthened RC beams exhibited a significant variation compared to the data from concrete prisms only. Furthermore, some of the presented data in the literature is not complete. Although the dataset used herein is considered relatively small, it demonstrated good reliability, which will be discussed in the proceeding section.

2.3 Data consistency analysis

Cronbach's alpha (α) is a statistical measure commonly used in research to assess the internal consistency of a data set intended to measure a variable. It quantifies the extent to which a set of items in a scale or questionnaire consistently measures the same underlying concept. Mathematically, Cronbach's alpha is calculated as the average of all possible split-half reliability coefficients, corrected for the number of items and the average inter-item correlation. The formula for Cronbach's alpha is expressed as:

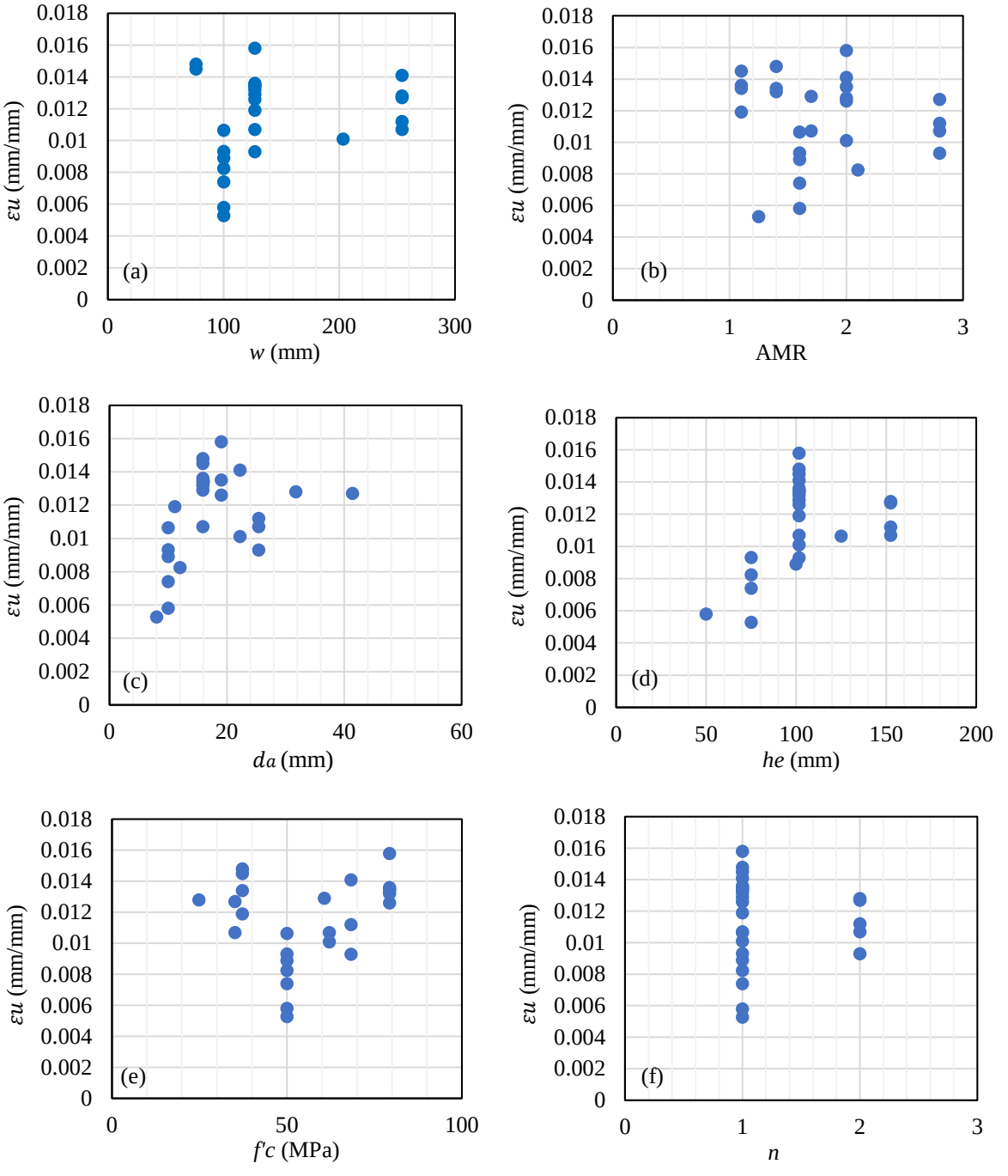

Fig. 3 Variation of strain with each tested parameter (a) Width of CFRP sheet; (b) Anchor's to sheet material ratio; (c) Anchor's dowel diameter; (d) Anchor's embedment depth; (e) Concrete compressive strength; (f) Number of CFRP sheets.

$$\alpha = \frac{N}{N-1} + \left(1 - \frac{\sum_{i=1}^{N} \sigma_i^2}{\sigma_x^2}\right) \quad (2)$$

where N is the number of observations, σ_i^2 is the variance of the *ith* item, and σ_x^2 is the variance of the total score.

Cronbach's alpha ranges from 0 to 1, with higher values indicating greater internal consistency among the items. A commonly accepted threshold for satisfactory reliability is a Cronbach's alpha of 0.70 or higher, Table 3 displayed the primary reliability and validity statistics for each component, including Cronbach's (α). The overall Cronbach's (α) was 0.805760, reflecting the good consistency for each of the key variables of this study.

Table 3. Data consistency measurements.

Factors	Correlation in Total	Cronbach's (α)
w	0.648203	0.755997
AMR	0.747033	0.732268
d_a	0.852489	0.705807
h_e	0.688723	0.746392
f'_c	-.114118	0.907303
n	0.725587	0.737504

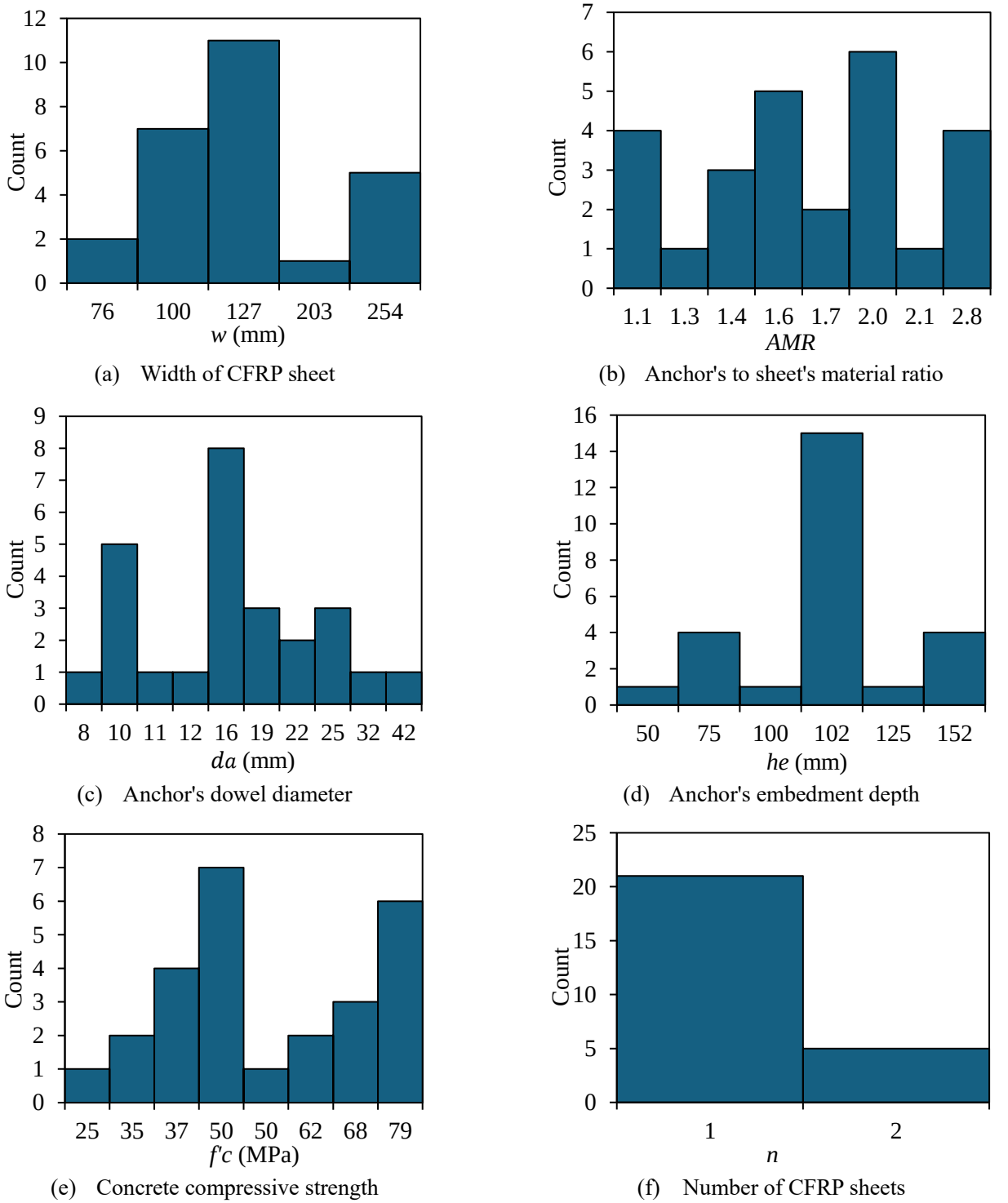

Fig. 4 Histogram of input variables (a) Width of CFRP sheet; (b) Anchor's to sheet material ratio; (c) Anchor's dowel diameter; (d) Anchor's embedment depth; (e) Concrete compressive strength; (f) Number of CFRP sheets.

Examining the dispersion or spread of data points within a dataset is a common step in an SAS variability analysis.[39] Measures of variability, including variance, mean, standard deviation, and more, were computed using PROC MEANS in SAS. As an interpretation of the variability analysis in SAS, PROC MEANS procedure in SAS was used to calculate statistical measures such as mean and standard deviation for the survey numerical variables (Table 4). A large variance or standard deviation indicates greater variability in the dataset.

2.4 Data correlation

Pearson's correlation coefficient, often denoted as r, is a statistical measure that quantifies the strength and direction of the linear relationship between two continuous variables. It ranges from -1 to 1, where: $r = 1$ indicates a perfect positive linear relationship, $r = -1$ indicates a perfect negative linear

Table 4. Mean and standard deviations.

Variable	N	Mean	Std Dev	Minimum	Maximum
w	26	143.2	59.97	76.2	254
AMR	26	1.790	0.54	1.10	2.80
d_a	26	17.66	7.684	8.00	41.4
h_e	26	104.2	25.45	50.0	152
f'_c	26	56.15	17.10	24.8	79.3
n	26	1.192	0.40	1.00	2.00

relationship, $r = 0$ indicates no linear relationship between the variables. The formula for Pearson's correlation coefficient between variables X and Y is given by:

$$r = \frac{\Sigma_{i=1}^{n}(X_i - \overline{X})(Y - \overline{Y})}{\sqrt{\Sigma_{i=1}^{n}(X_i - \overline{X})^2 \Sigma_{i=1}^{n}(Y_i - \overline{Y})^2}} \quad (3)$$

where n is the number of paired observations, Xi and Yi are the individual values of variables X and Y, $\overline{X}$ and $\overline{Y}$ are the means of variables X and Y, respectively. A Pearson correlation matrix, often displayed as a heatmap, visually represents the correlation coefficients between multiple variables. Each cell in the matrix represents the correlation between two variables, with values closer to 1 indicating a stronger positive correlation, values closer to -1 indicating a stronger negative correlation, and values close to 0 indicating little to no correlation. The diagonal of the matrix typically displays perfect correlation (r=1), as each variable correlates perfectly with itself.

The heatmap in Fig. 5 illustrates the correlation between various parameters, represented by the shades of color corresponding to the correlation coefficient values ranging from -1 to 1. In this matrix, darker teal shades indicate a stronger positive correlation, meaning as one parameter increases, the other also tends to increase. Conversely, the lighter cream and beige colors represent a negative correlation, signifying that an increase in one parameter is associated with a decrease in the other. The cells that are closer to white denote a correlation near zero, suggesting no linear relationship between those parameters. A negative correlation between ε_u with w is noticed, implying that as the width increases, the strain at ultimate load tends to decrease as well. Similarly, AMR has a slight negative correlation with the ultimate strain. It should be noted that the previously published data did not seem to draw a clear relationship between AMR and the strain. Conversely, d_a and h_e seem to have a positive influence on the value of the ultimate strain. This is true since increasing the dowel diameter and embedment depth means heavier anchorage, leading to higher strain utilization. The concrete compressive strength (f'_c) is shown to have a negligible effect on the strain and almost no correlation with other parameters. The number of layers (n) is considered a categorical variable, meaning that its value indicates a distinct category or group rather than a continuous spectrum. The number of layers does not correlate linearly with ε_u or other parameters; instead, it delineates different configurations or arrangements within the laminates. The effect of the number of layers will be further illustrated in the proposed prediction model in section 3.

2.5 Prediction models

Since the dataset is relatively small, the focus is on simplicity, efficiency, and suitability for small datasets. Linear models are particularly suitable when the relationship between the input and output variables is expected to be approximately linear. Their simplicity also allows for straightforward interpretation and faster training times, which are crucial in scenarios with limited data. Linear regression and linear SVR are both simple and efficient modeling techniques. Given the small dataset, these models are appropriate because they are less likely to overfit than more complex models. Decision trees are included as an exploratory approach to capture potential nonlinear relationships between features and the target variable. Unlike linear models, decision trees do not require the assumption of linearity and can model complex interactions between features

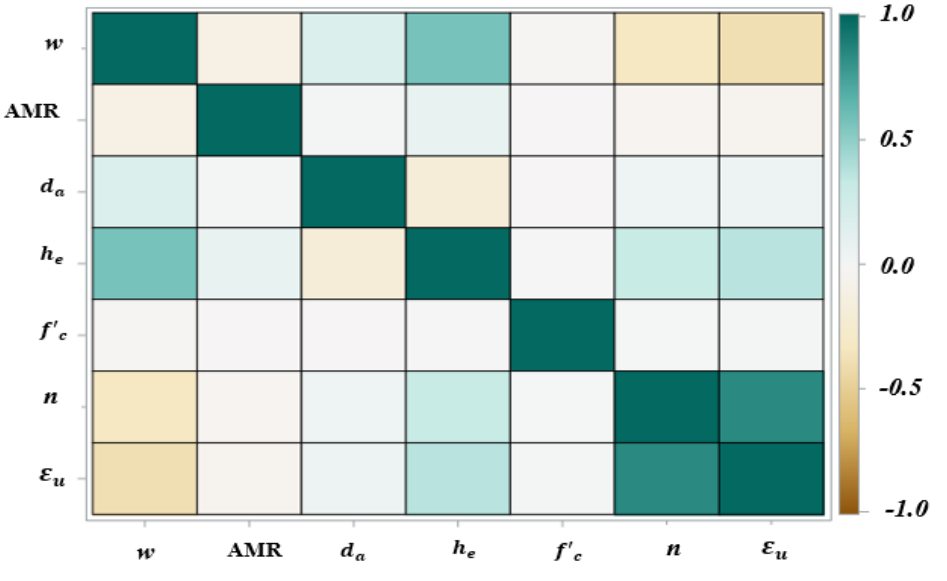

Fig. 5 Heatmap of correlation coefficients between input and output variables.

with a straightforward, hierarchical structure. All three models-linear regression, linear SVR, and decision trees-can perform reasonably well with smaller datasets. They have relatively low requirements for sample size to achieve stable estimates, making them suitable choices for a dataset of less than 30 data points. Using these models can also serve as a baseline for modeling performance. If more complex models are considered in the future, comparisons with the results from these simpler models can help assess whether the additional complexity is justified.

2.5.1 Linear regression

Linear regression is a foundational statistical method extensively used in scientific research across various disciplines, from social sciences to engineering. It is a fundamental tool for understanding the relationship between a dependent variable and one or more independent variables. In scientific studies, researchers often aim to understand how changes in one or more independent variables influence the outcome of interest, which is the dependent variable. Linear regression assumes a linear relationship exists between the independent and dependent variables. This implies that changes in the independent variables lead to proportional changes in the dependent variable. A simple linear regression equation describes the relationship:

$$Y = \beta_0 + \sum_{i=1}^{n}(\beta_i X_i) + \epsilon \quad (4)$$

where Y is the dependent variable, X_i is the independent variable, β_0 is the intercept, β_i is the correlation coefficient related to variable X_i, n is the total number of independent variables and ϵ represents the error term. The coefficient (β_i) in the regression equation represents the change in the dependent variable for a one-unit change in the corresponding independent variable, holding other variables constant. The intercept (β_0) represents the value of the dependent variable when all independent variables are zero. Measures such as R2 (coefficient of determination) are used to measure the goodness of fit, which indicates the proportion of variance explained by the model.

In linear regression analysis, several assumptions underlie the validity of the model. Firstly, linearity assumes that a straight line can adequately represent the relationship between the independent and dependent variables. This implies that changes in the independent variable result in proportional changes in the dependent variable. Secondly, homoscedasticity posits that the variance of the errors remains constant across all levels of the independent variables, indicating that the spread of the residuals around the regression line is consistent. Lastly, normality of errors assumes that the errors, or residuals, are normally distributed with a mean of zero. This means that the distribution of the residuals follows a bell-shaped curve, allowing for reliable inference and hypothesis testing. These assumptions collectively form the basis for assessing the reliability and accuracy of linear regression models and are essential considerations in interpreting the results and making valid conclusions. Violations of these assumptions can lead to biased parameter estimates and erroneous inferences, underscoring the importance of thorough diagnostic checks and, if necessary, applying appropriate corrective measures.

2.5.2 Linear SVR

Linear Support Vector Regression (SVR) is a version of Support Vector Machine (SVM) designed for regression tasks that aim to find the hyperplane that has the maximum number of points within a certain threshold (ε) from the actual linear line it predicts. The ε-insensitive loss function is what differentiates SVR from other regression models. This function does not penalize errors within the margin of ε from the true value, which helps manage within the margin of ε from the true value, which helps manage the outliers and makes the model robust. This method aims to balance minimizing errors, keeping the model simple in training data, and keeping the model applicable across scenarios. The regularization parameter in the model's loss function plays a role in maintaining this balance, impacting both error reduction and model simplicity. Mathematically, the optimization problem for linear SVR can be formulated as:

$$\min_{w,b} \frac{1}{2}||w||^2 + C\sum_{i=1}^{n}(\xi_i + \xi_i^*) \quad (5)$$

Subject to the constraint for each data point i:

$$y_i - \langle w, x_i\rangle - b \leq \epsilon + \xi_i \quad (6)$$

$$\langle w, x_i\rangle + b - y_i \leq \epsilon + \xi_i^* \quad (7)$$

where w is the weight vector of the hyperplane, b is the bias term, x_i and y_i are the feature vector and target value, respectively, of the i-th data point, ξ_i and ξ_i^* are slack variables that measure the degree of violation of the ε-insensitive loss for points above and below the ε-tube, respectively. C is the regularization parameter that controls the trade-off between the flatness of the hyperplane and the amount up to which deviations larger than ε are tolerated, ϵ is the margin of tolerance where no penalty is given to errors. To solve the Linear SVR optimization problem, it is often transformed into its dual form, enabling the use of kernel tricks for nonlinear regression tasks. However, Linear SVR focuses on linear kernels, where the relationship between the feature space and target values is linear. In this context, support vectors become a pivotal aspect of the model. These support vectors are the data points that lie outside the ε-insensitive zone or exactly on its boundary, significantly influencing the position and orientation of the hyperplane. Conversely, Data points within the ε-margin do not impact the model's predictions. This characteristic underscores Linear SVR's efficiency, especially when the input features and the target variable share a roughly linear relationship. This process allows for an assessment using metrics, like squared error (MSE) and coefficient of determination (R^2) to gauge how accurately the model predicts outcomes and fits the data. The model's resilience against outliers and its capability to manage model complexity through regularization, renders Linear SVR a highly adaptable tool for regression analyses.

2.5.3 Decision trees

Decision trees are a non-parametric supervised learning method for classification and regression tasks. The goal is to create a model that predicts the value of a target variable by learning simple decision rules inferred from the data features. In addressing the regression dataset, a Decision Tree algorithm was deployed to capture the relationship between predictor variables and the continuous outcome variable. Decision Trees divide the dataset into groups based on the input feature values to ensure that similar target values are grouped in each subset. A decision tree consists of a root node, the first node of the tree where the data is split, into decision nodes, the subsequent nodes where further splits occur, and leaf nodes, which do not split further and contain the output values. The steps to build a regression tree start at the root node, where the entire dataset is inserted. The algorithm considers all possible values for each feature to split the data into two groups. The best split is determined using a criterion such as MSE. The aim is to find the split that results in the highest reduction in variance. The MSE for a potential split is calculated as follows:

$$MSE_{split} = \frac{n_{left}}{N} MSE_{left} + \frac{n_{right}}{N} MSE_{right} \quad (8)$$

where n_{left} and n_{right} are the number of observations in the left and right splits, N is the total number of observations, and MSE_{left} and MSE_{right} are the MSEs of the left and right splits, respectively. After that, the best feature and value to split on becomes a decision node. If a stopping criterion (such as a minimum number of samples to make a split, maximum tree depth, or minimal reduction in MSE) is met, the current node becomes a leaf node. Once a leaf node is reached, it is assigned an output value. For regression trees, this is often the mean target value of the samples within the leaf. The tree may be pruned by removing branches with little predictive power to avoid overfitting.

2.5.4 Model comparison

A comparative analysis of the three prediction models utilized in this study is presented herein. The models' performance evaluation is based on two key metrics: coefficient of determination (R^2) and root mean squared error (RMSE). These metrics are crucial for understanding how well each model predicts actual outcomes and how much error is involved in these predictions. R^2 measures the proportion of the variance in the dependent variable that is predictable from the independent variables. It indicates the model's goodness of fit. The R^2 value ranges from 0 to 1, where a value closer to 1 indicates that the model explains much of the variance. The equation for R^2 is:

$$R^2 = 1 - \frac{\sum_{i=1}^{n}(y_i - \hat{y}_i)^2}{\sum_{i=1}^{n}(y_i - \bar{y})^2} \quad (9)$$

where y_i is the actual value for the ith observation, $\hat{y}_i$ is the predicted value of the ith observation, $\bar{y}$ is the mean of actual values, and n is the total number of observations. The numerator $\sum_{i=1}^{n}(y_i - \hat{y}_i)^2$ is the sum of the squared differences between the actual and predicted values, representing the unexplained variance. The denominator $\sum_{i=1}^{n}(y_i - \bar{y})^2$ is the total sum of the squares of the differences between the actual values and their mean, representing the total variance.

RMSE measures the average magnitude of the errors between the actual and predicted values, providing a sense of how far, on average, the predictions are from the actual values. The calculation for RMSE is presented in Eq. 8. The term $\sum_{i=1}^{n}(y_i - \hat{y}_i)^2$ calculates the sum of the squared differences between the actual and predicted values. Dividing this sum by the total number of observations (n) calculates the MSE. The square root of MSE gives the RMSE, which is in the same units as the dependent variable, making it a valuable measure of error magnitude. A lower RMSE indicates a model with lower average prediction errors, suggesting more accurate predictions.

$$RMSE = \sqrt{\frac{1}{n}\sum_{i=1}^{n}(y_i - \hat{y}_i)^2} \quad (10)$$

Furthermore, Multiple random splits were used to create the training and testing datasets. The average performance metrics, such as R^2 and RMSE were calculated across these iterations, providing insights into the model's consistency and reliability on new and previously seen data. This approach helped reduce bias in performance assessment and indicated the model's ability to generalize to new data.

Figure 6 demonstrates R^2 and *RMSE* for each model. Based on R^2, linear regression shows the highest predictive accuracy among the three models, followed closely by decision trees and linear SVR. In terms of prediction error measured by *RMSE*, linear regression has the lowest error, indicating its predictions are closest to the actual values. Decision trees and linear SVR have higher errors, with linear SVR having the highest error rate. This comparative analysis reveals that linear regression best balances accuracy and prediction error among the three models. Therefore, this model was chosen to provide a predictive equation for the ultimate strain in the CFRP laminates, as explained in the proceeding section.

Figure 7 illustrates the predicted versus actual values for each model. The plot of predicted versus actual values will typically show a linear relationship if the model performs well. The points should lie close to the diagonal line representing perfect predictions (where predicted values equal actual values). It can be observed that the linear regression model provides the closest prediction compared to linear SVR and decision trees model, as the scatter of points is distributed close to the unity line in linear regression. This can be attributed to the small size of the dataset used. Linear regression's effectiveness in providing close predictions compared to linear SVR and decision trees can be attributed to several factors. Firstly, its reliance on the assumption of a linear relationship between independent and dependent variables favours datasets where such relationships are predominant; however, this needs further validation with additional datasets. Moreover, linear regression's simplicity in modelling the relationship between variables makes it particularly suitable for small datasets with limited observati-

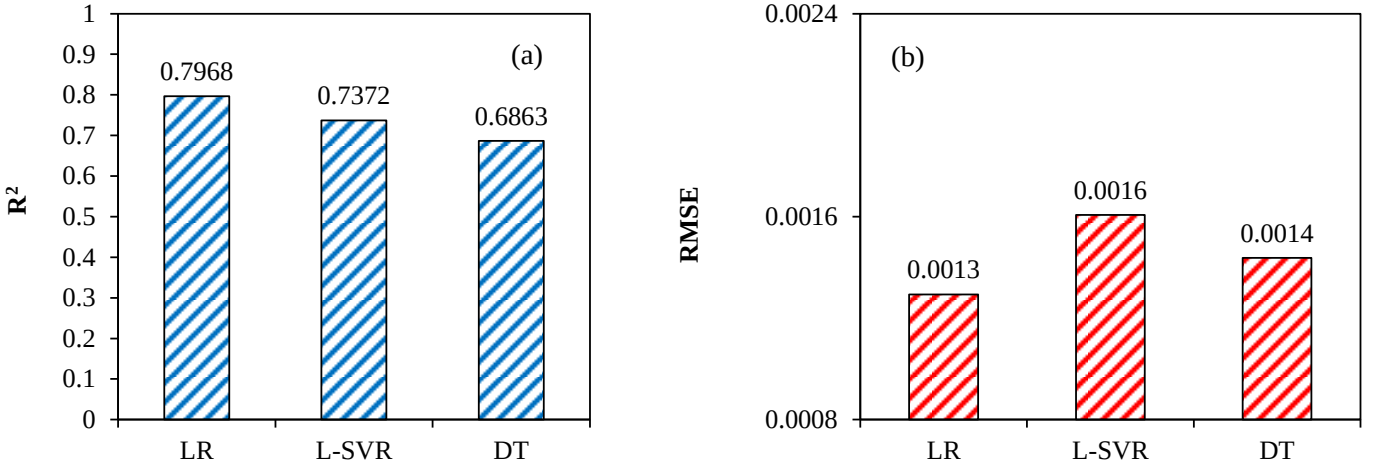

Fig. 6 Comparison of performance measures for the three models (a) R^2; (b) RMSE.

ons. Additionally, the robustness of linear regression against outliers plays a crucial role, especially in small datasets where outliers can disproportionately influence model performance. Linear regression's ability to handle outliers more gracefully contributes to its ability to provide reliable predictions in such scenarios.

As a result of the overall comparison of the developed models, it can be observed that linear regression models offer simplicity, ease of interpretation, and explicit predictive equations, making them efficient for small datasets to establish data-driven design relations/diagrams. However, such models assume linear relations between input and output variables and disregard complex or nonlinear patterns within the data. Therefore, more sophisticated models were investigated, *i.e.* Linear SVR and decision trees. Linear SVR, although linear, offers robustness and regularization that can enhance performance over ordinary linear regression, especially with high-dimensional data. On the other hand, decision trees capture interactions and complex patterns, providing feasible visualizations and interpretations. Despite their advantages, linear SVR requires parameter tuning and sufficient datasets to support the tuning for high performance in the prediction, and decision trees are prone to overfitting, particularly with small datasets. The performance metrics used in this study reflect these characteristics. However, the developed algorithm is dynamic, allowing ongoing comparisons and updates as new data points are added. The combination of these factors underscores the effectiveness of linear regression in scenarios where dataset size is limited, offering a compelling alternative to more complex models like linear SVR and decision trees.

2.6 Proposed prediction model

After ensuring the appropriateness of the linear regression framework for the given data, a predictive linear equation of the ultimate strain (ε_u) is proposed in this section using SAS.[39] Table 5 provides the coefficients corresponding to each parameter in the equation, expressing the statistical significance of the parameter. Stepwise regression was utilized to retain only the significant variables with p-value < 0.05. The p-values for all parameters, except for the concrete compressive strength (f'_c), being less than 0.05 indicates a statistically significant relationship between these variables and the maximum strain in the linear regression model. This implies a high confidence level in asserting that changes in the number of layers, *AMR*, dowel diameter, and embedment depth, are associated with significant variations in the maximum strain. The larger p-value for the concrete compressive strength suggests that this variable may not be as influential in predicting maximum strain as the other factors. However, concrete compressive strength influences the debonding strain according to ACI 440-19,[35], i.e. the strain at which the FRP laminate detaches from the concrete substrate. The larger p-value for this variable is due to the limited range of compressive strength values in the data collected.

Table 5. Characteristics of proposed model to predict ultimate strain in anchored FRP laminates.

Variable	Coefficient	Standard error	T value
w	-0.000282	0.00009	-3.11
AMR	-0.001803	0.001172	-1.54
d_a	0.005767	0.001215	4.75
h_e	0.000749	0.000252	2.97
n	0.007322	0.001785	4.1
Intercept	-0.00524	0.004052	-1.29

Based on the results in Table 5, the predicted maximum strain is presented by Eq. 11:

$$\varepsilon_u = -0.00028w - 0.0018AMR + 0.005767d_a + 0.000749h_e + 0.007322n - 0.00524 \quad (11)$$

(w, d_a, n and h_e in cm)

As for the sign of the estimates, the positive signs for most of the coefficients, including the number of layers, *AMR*, dowel diameter, and embedment depth, signify a positive correlation with the maximum strain. This means that an

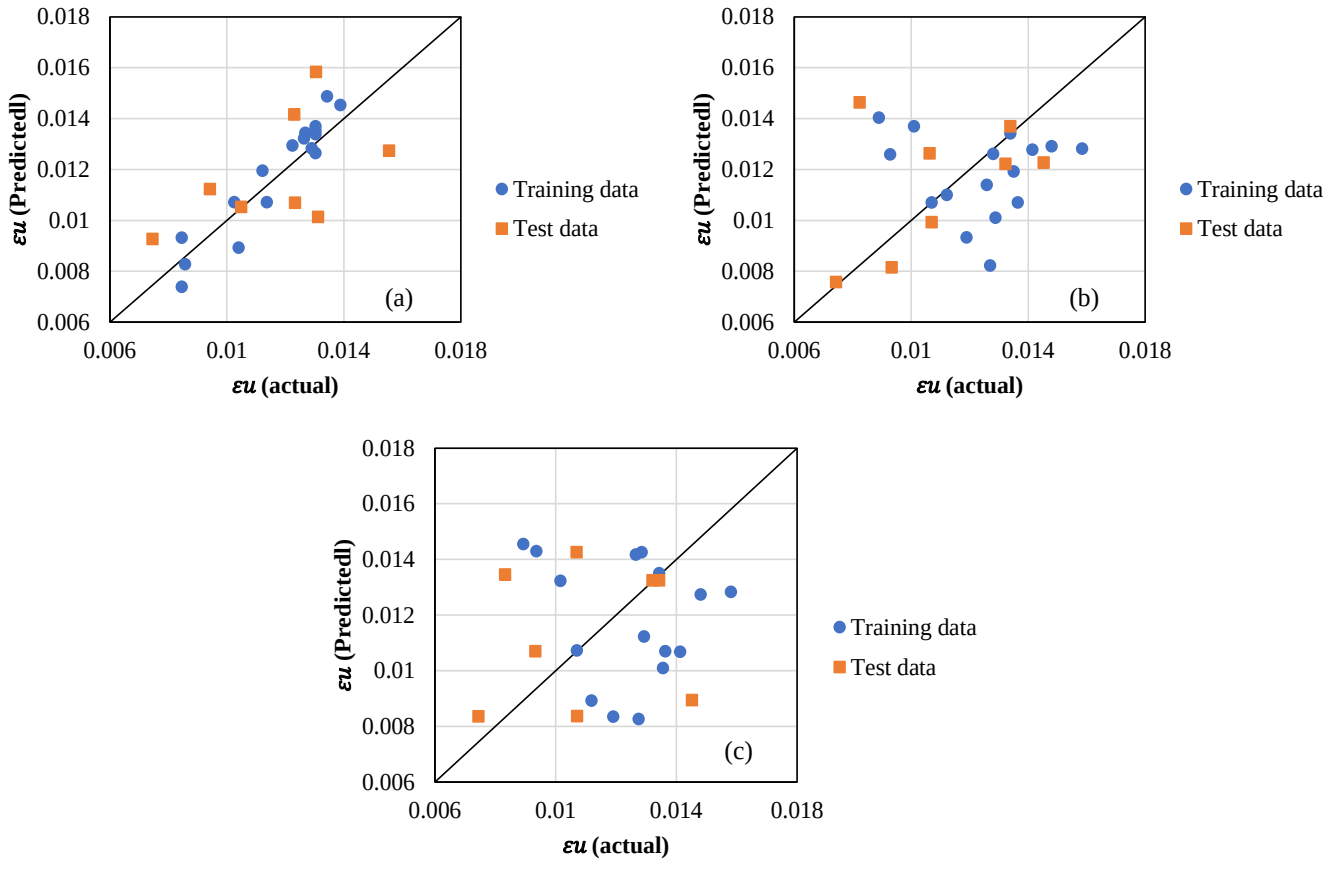

Fig. 7 Predicted versus actual strains for each model (a) Linear regression model; (b) Linear SVR; (c) Decision trees.

increase in these variables is associated with an increase in maximum strain. On the contrary, the negative sign for the width variable suggests a negative correlation, indicating that an increase in width is associated with a decrease in maximum strain. This could be justified, considering that wider laminates have uneven and higher range of stresses within the FRP sheet, leading to lower maximum strain values.

In linear regression, residuals represent the differences between the observed values of the dependent variable and the values predicted by the regression model. These differences, or errors, are essential for assessing how well the model fits the data. Residuals are calculated by subtracting the predicted values *Yi* from the observed values *Yi*^ for each data point, where *Yi* represents the observed value of the dependent variable for data point *i*, and *Yi*^ represents the predicted value of the dependent variable for data point *i*. The residuals represent the performance of the regression model. Ideally, the residuals should be small and evenly distributed around zero, indicating that the model captures the underlying relationships in the data well. However, if the residuals exhibit patterns or large deviations from zero, it suggests that the model may not adequately explain the variability in the data. Residual plots, such as scatterplots of residuals against predicted values or independent variables, are commonly used to visually inspect the residuals for patterns. Fig. 8 shows the scatter plot of the residuals, which are randomly distributed and confirms that the model is good. Further, Table 6 shows the discrepancy between the actual and predicted values according to Eq. 11-14 and the corresponding percentage error. It can be seen that the maximum value of discrepancy is 0.00528, and the average

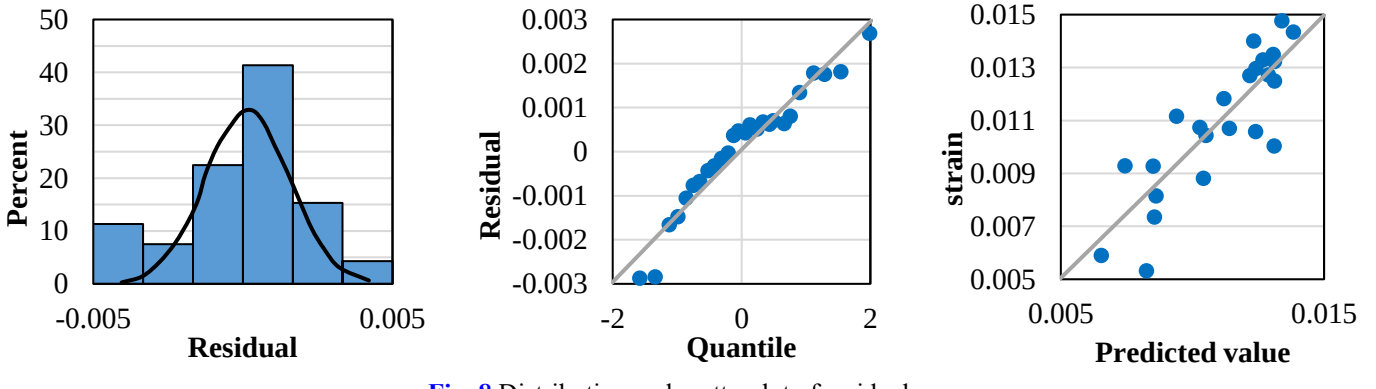

Fig. 8 Distribution and scatterplot of residuals.

Table 6. Comparison between predicted and actual strains.

w (mm)	AMR	d_a (mm)	h_e (mm)	n	Actual ε_u (mm/mm)	Predicted ε_u (mm/mm)	Discrepancy	%Error
76.20	1.40	15.88	101.6	1	0.0148	0.0142	-0.00061	-4.13%
76.20	1.10	15.88	101.6	1	0.0145	0.0147	0.00023	1.59%
127	1.70	15.88	101.6	1	0.0129	0.0122	-0.00067	-5.23%
203.2	2.00	22.23	101.6	1	0.0101	0.0132	0.003113	30.83%
254	1.70	15.88	101.6	1	0.0107	0.0087	-0.00203	-18.97%
127	2.80	25.40	101.6	2	0.0093	0.008414	-0.00089	-9.53%
254	2.00	22.23	101.6	1	0.0141	0.011791	-0.00231	-16.38%
254	2.80	25.40	152.4	2	0.0112	0.008663	-0.00254	-22.66%
127	2.80	25.40	152.4	2	0.0107	0.012219	0.001519	14.19%
254	2.80	41.40	152.4	2	0.0127	0.017891	0.005191	40.87%
254	2.00	31.75	152.4	2	0.0128	0.013767	0.000967	7.55%
127	2.00	19.05	101.6	1	0.0135	0.0135	1.6E-05	0.12%
127	1.40	15.88	101.6	1	0.0132	0.0128	-0.00043	-3.28%
127	1.10	15.88	101.6	1	0.0136	0.0133	-0.00029	-2.15%
127	1.10	11.11	101.6	1	0.0119	0.0106	-0.00134	-11.25%
127	1.10	15.88	101.6	1	0.0134	0.0133	-9.2E-05	-0.69%
127	2.00	19.05	101.6	1	0.0126	0.0135	0.000916	7.27%
127	1.40	16.00	101.6	1	0.0134	0.0128	-0.00056	-4.18%
127	2.00	19.05	101.6	1	0.0158	0.0135	-0.00228	-14.46%
100	1.60	9.98	75	1	0.0074	0.0078	0.000362	4.89%
100	1.25	8.00	75	1	0.0053	0.0073	0.001979	37.47%
100	2.10	11.99	75	1	0.0082	0.0080	-0.00022	-2.63%
100	1.60	9.98	50	1	0.0058	0.0059	9.79E-05	1.69%
100	1.60	9.98	100	1	0.0089	0.0096	0.000748	8.41%

value of the discrepancy between the actual and predicted strains is 0.001314. Moreover, the highest error percentage depicted in the table is 40%, with an absolute average of 1.19%. These values are relatively low, which indicates the ability of equations 11-14 to predict the maximum strain in the FRP laminate.

3. Design of CFRP anchors

In this section, specified values were suggested for the influential parameters in equations 11 and 13 (w, AMR, d_a, h_e, and n). Equations 11 and 13 were solved using MATLAB. The algorithm begins by generating a grid of parameter combinations using equally spaced values for the parameters used. Then, it calculates the strain values based on these combinations Eq. 11, then filters out combinations that fall within a specified range of strain values. The chosen strain values in this study were 0.006, 0.008, 0.01, and 0.012. It should be noted that a higher ultimate strain value is preferred but requires more anchorage (*i.e.* larger dowel diameter, higher embedment depth, or more anchors). The filtered combinations are stored for further analysis. Finally, it applies additional criteria to remove combinations that do not meet certain requirements, ensuring that only valid combinations are retained for further investigation. The requirements specified for this algorithm are the limits (minimum and maximum) for each parameter, and the relationships between the parameters, for instance, a condition on the embedment depth is set to be 6 to 10 times the dowel diameter. Moreover, increments were specified for each parameter to match the practical considerations. The defined parameter space limits are w :(50 - 300) mm with increments of 25 mm, AMR: (1-3) with increments of 0.1, d_a: (8 - 24) mm with increments of 1 mm, and h_e: (50-300) mm with increments of 5 mm. The combinations of parameters that satisfy strain values of (0.006, 0.008, 0.01, 0.012) in Eq. were determined. As a result of the analysis, 13161 combinations for Eq. 11 were determined. Therefore, the results had to be filtered according to the following criteria. First, the number of anchors needed to satisfy a certain combination was determined using the AMR equation mentioned in section 2.2 (Eq. 1), assuming the thickness of the FRP laminate to be 0.5 and 1 mm (most common commercial sizes). When the number of anchors exceeded 4, the combination was excluded. Also, a lesser number of anchors is preferred. Since it is not possible to list all applicable combinations herein, only the combinations corresponding to an AMR of 2.2 and 1.1 were chosen. Sun *et al.*[27] and Alotaibi *et al.*[33] recommended a minimum AMR of 2 and 2.2, respectively. However, few studies have shown that an AMR of less than 2 still provides proper anchorage.[29]

Figure 9 illustrates the design charts plotted from the analysis of the proposed strain equation (Eq. 11). The charts provide a design guide for strengthened and anchored concrete beams regarding the width of the FRP sheet (w), the required

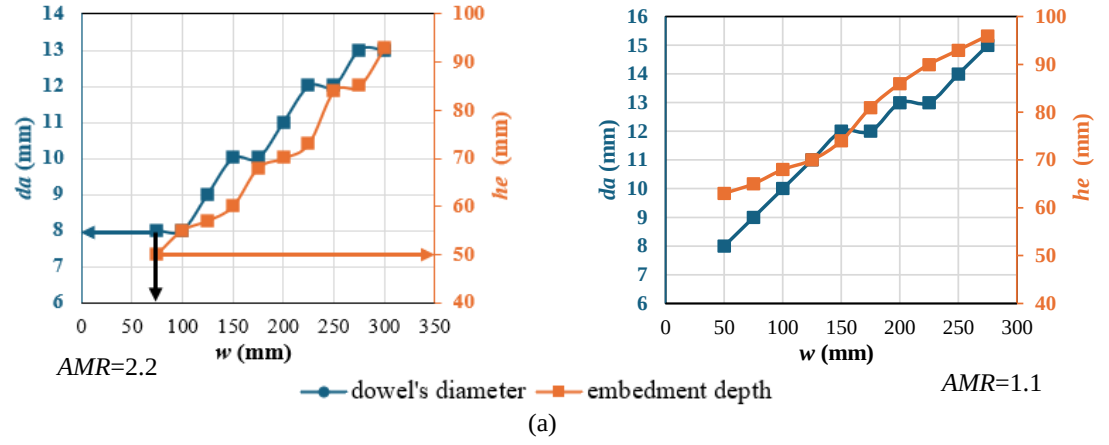

(a)

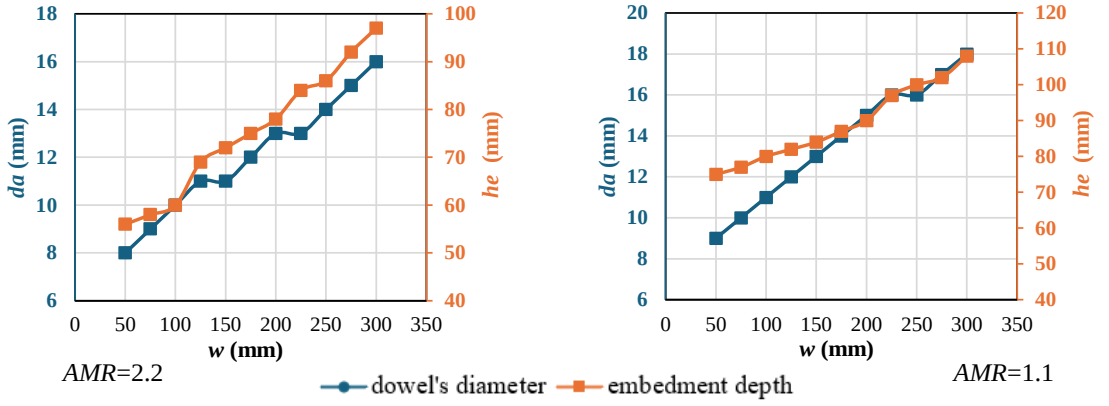

(b)

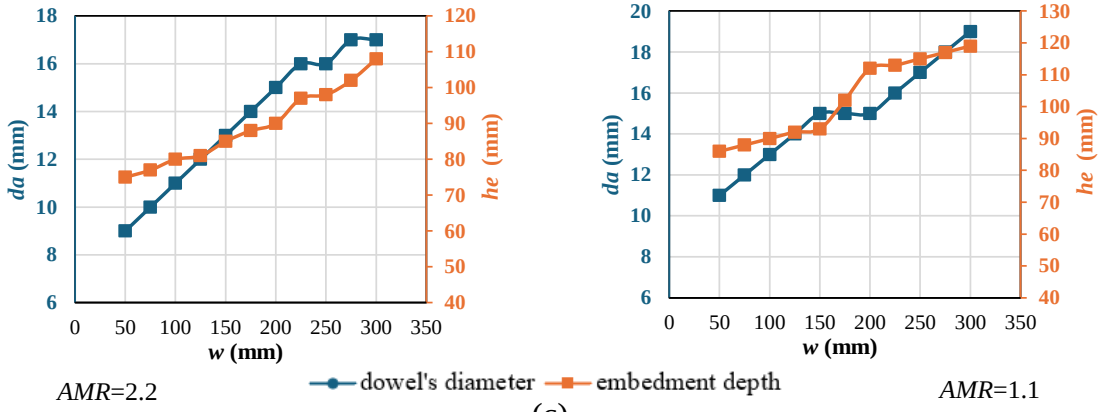

(c)

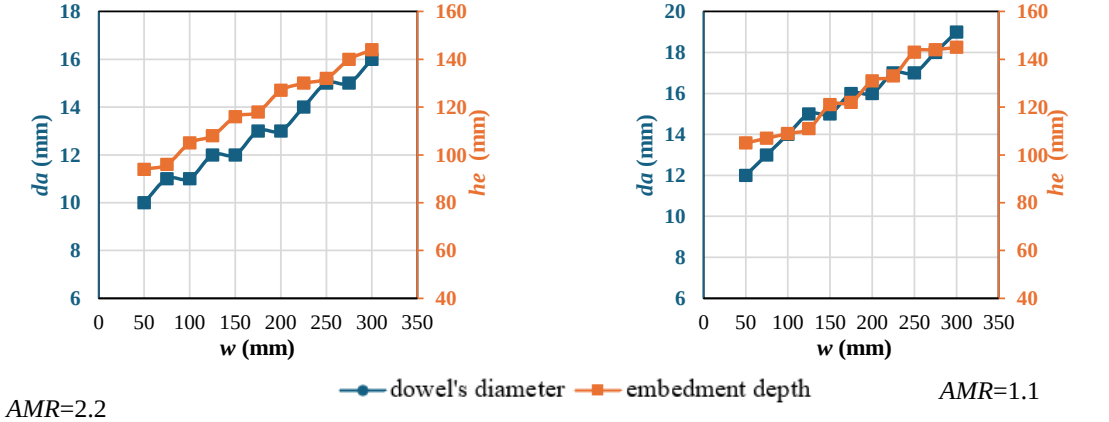

(d)

Fig. 9 Design charts for strengthened and anchored concrete beams (a) ε_u=0.006. (b) ε_u=0.008. (c) ε_u=0.01. (d) ε_u=0.012.

anchor's dowel diameter (d_a), and the required anchor's embedment depth (h_e) to satisfy a certain ultimate strain value (0.006, 0.008, 0.01, and 0.012 as shown in Fig. 9a to 9d, respectively). For instance, to obtain a strain value of 0.006 for an FRP laminate of 75 mm width, satisfying an AMR of 2.2, the anchor's dowel diameter should be 8 mm, and the embedment depth should be 50 mm, as indicated in Fig. 9a.

4. Conclusions

The data analysis conducted in this study aimed to understand the relationship between various key parameters and the maximum strain observed in strengthened and anchored concrete beams. Multiple models for regression analysis were employed, including machine learning-based models and traditional linear regression. The following conclusions can be derived from this study:

- Linear regression was found to be the most capable model for predicting the ultimate strain in the FRP laminates using the given dataset. Parameters considered were the width of the FRP sheet (w), anchor's to sheet material ratio (AMR), anchor's dowel diameter (d_a), anchor's embedment depth (h_e) and the number of FRP layers (n).
- Measurement reliability was assessed using Cronbach's (α), indicating a good internal consistency of the dataset. The analysis of variability using SAS highlighted the spread of data points within the dataset.
- The prediction model constructed through linear regression allowed for a comprehensive examination of the relationships between the maximum strain and the input variables. The examination of residuals confirmed the suitability of the linear regression framework for the dataset, and the estimates and p-values provided a detailed understanding of the statistical significance of each predictor.
- Based on the results, predictive equations were derived for the maximum strain, incorporating the significant variables identified through linear regression analysis. The R-squared value of 0.81 indicated a good fit of the regression model to the data, and the p-values suggested statistically significant relationships between most predictors and the maximum strain.
- The proposed model was employed to provide design charts and recommendations for the anchor's parameters that yield specific maximum strain values. Furthermore, the design charts take into account practical implementation considerations and adhere to previously recommended limits on AMR and anchor's diameter-to-depth ratio.

Acknowledgements

The support for the paper's publication was provided by the American University of Sharjah through Riad T. Sadek, the endowed chair of the Civil Engineering and Open Access Program (OAP). The support is gratefully acknowledged and appreciated. The views and conclusions expressed or implied are those of the authors and should not be interpreted as those of the donor or the institution.

Conflict of Interest

There is no conflict of interest.

Supporting Information

Not applicable.

References

[1] B. AL-Eliwi, N. Sheet, R. Najem, W. Hasan, The optimum design of RC beams strengthened with FRP materials: a review, *Al-Rafidain Engineering Journal (AREJ)*, 2023, **28**, 18-32, doi: 10.33899/rengj.2023.139008.1244.

[2] A. Jahami, C. A. Issa, An updated review on the effect of CFRP on flexural performance of reinforced concrete beams, *International Journal of Concrete Structures and Materials*, 2024, **18**, 14, doi: 10.1186/s40069-023-00651-y.

[3] R. A. Hawileh, M. A. Assad, J. A. Abdalla, M. Z. Naser, Finite element modeling of reinforced concrete beams externally bonded with PET-FRP laminates, *Computers and Concrete*, 2024, **33**, 163–173, doi: 10.12989/cac.2024.33.2.163.

[4] S. P. Kaliyappan, P. Pakkirisamy, Behavior of reinforced concrete beam with CFRP and GFRP laminates, *Matéria (Rio De Janeiro)*, 2023, **28**, doi: 10.1590/1517-7076-rmat-2023-0222.

[5] K. Sengun, G. Arslan, Performance of RC beams strengthened in flexure and shear with CFRP and GFRP, *Iranian Journal of Science and Technology, Transactions of Civil Engineering*, 2024, **48**, 117-130, doi: 10.1007/s40996-023-01305-5.

[6] H. S. Mahmoud, R. A. Hawileh, J. A. Abdalla, Strengthening of high strength reinforced concrete thin slabs with CFRP laminates, *Composite Structures*, 2021, **275**, 114412, doi: 10.1016/j.compstruct.2021.114412.

[7] K. Dong, Y. Gao, S. Yang, Z. Yang, J. Jiang, Experimental investigation and analytical prediction on bond behaviour of CFRP-to-concrete interface with FRP anchors, *Case Studies in Construction Materials*, 2023, **19**, e02510, doi: 10.1016/j.cscm.2023.e02510.

[8] M. Assad, R. Hawileh, J. Abdalla, Finite element simulation of FRP-strengthened thin RC slabs, *Journal of Composites Science*, 2022, **6**, 263, doi: 10.3390/jcs6090263.

[9] N. Attari, S. Amziane, M. Chemrouk, Flexural strengthening of concrete beams using CFRP, GFRP and hybrid FRP sheets, *Construction and Building Materials*, 2012, **37**, 746-757, doi: 10.1016/j.conbuildmat.2012.07.052.

[10] M. E. Uz, Y. Guner, E. Avci, Strengthening of reinforced concrete beams via CFRP orientation, *Buildings*, 2023, **14**, 82, doi: 10.3390/buildings14010082.

[11] A. F. Ashour, S. A. El-Refaie, S. W. Garrity, Flexural strengthening of RC continuous beams using CFRP laminates, *Cement and Concrete Composites*, 2004, **26**, 765-775, doi: 10.1016/j.cemconcomp.2003.07.002.

[12] M. M. Önal, Strengthening reinforced concrete beams with CFRP and GFRP, *Advances in Materials Science and Engineering*, 2014, **2014**, 967964, doi: 10.1155/2014/967964.

[13] A. Ali, J. Abdalla, R. Hawileh, K. Galal, CFRP mechanical anchorage for externally strengthened RC beams under flexure,

Physics Procedia, 2014, **55**, 10-16, doi: 10.1016/j.phpro.2014.07.002.
[14] M. Assad, H. Mhanna, R. A. Hawileh, J. A. Abdalla, Finite element modeling of strengthened T-beams with CFRP U-wrapsAIP Conference Proceedings, The 2nd young scholar symposium on science and mathematics education, and environment. Bandar Lampung, Indonesia. AIP Publishing, 2024.
[15] J. A. Abdalla, H. H. Mhanna, A. B. Ali, R. A. Hawileh, CFRP U-wraps and spike anchors for enhancing the flexural performance of CFRP-plated RC beams, *Polymers*, 2023, **15**, 1621, doi: 10.3390/polym15071621.
[16] H. H. Mhanna, R. A. Hawileh, J. A. Abdalla, Shear behavior of RC T-beams externally strengthened with anchored high modulus carbon fiber-reinforced polymer (CFRP) laminates, *Composite Structures*, 2021, **272**, 114198, doi: 10.1016/j.compstruct.2021.114198.
[17] S. V. Grelle, L. H. Sneed, Review of anchorage systems for externally bonded FRP laminates, *International Journal of Concrete Structures and Materials*, 2013, **7**, 17-33, doi: 10.1007/s40069-013-0029-0.
[18] A. Mostafa, A. G. Razaqpur, CFRP anchor for preventing premature debonding of externally bonded FRP laminates from concrete, *Journal of Composites for Construction*, 2013, **17**, 641-650, doi: 10.1061/(asce)cc.1943-5614.0000377.
[19] H. Akbarzadeh Bengar, A. Ali Shahmansouri, A new anchorage system for CFRP strips in externally strengthened RC continuous beams, *Journal of Building Engineering*, 2020, **30**, 101230, doi: 10.1016/j.jobe.2020.101230.
[20] W. Sun, Development of a testing methodology for the design and quality control of carbon fiber reinforced polymer (CFRP) anchors, *Construction and Building Materials*, 2018, **164**, 150-163, doi: 10.1016/j.conbuildmat.2017.12.192.
[21] T. Ozbakkaloglu, M. Saatcioglu, Tensile behavior of FRP anchors in concrete, *Journal of Composites for Construction*, 2009, **13**, 82-92, doi: 10.1061/(asce)1090-0268(2009)13: 2(82).
[22] S. J. Kim, S. T. Smith, Behaviour of handmade FRP anchors under tensile load in uncracked concrete, *Advances in Structural Engineering*, 2009, **12**, 845-865, doi: 10.1260/136943309790327716.
[23] P. Villanueva Llauradó, J. F. Gómez, F. J. González Ramos, Influence of the anchor fan position on the performance of FRP anchors. D. A. Hordijk, M. Luković, eds. High Tech Concrete: Where Technology and Engineering Meet. Cham: Springer International Publishing, 2017.
[24] S. J. Kim, S. T. Smith, Pullout strength models for FRP anchors in uncracked concrete, *Journal of Composites for Construction*, 2010, **14**, 406-414, doi: 10.1061/(asce)cc.1943-5614.0000097.
[25] J. L. Jiménez, H. Santa María, Finite element analysis of the influence of dowel angle on CFRP anchors, *Composite Structures*, 2024, **331**, 117866, doi: 10.1016/j.compstruct.2023.117866.
[26] H. Zhou, Y. Yang, K. Liu, T.-L. Huang, Y. Ou, S. S. Zhang, Analytical study on the behavior of CFRP-concrete bonded joint with a non-rigid end-anchor, *Composite Structures*, 2023, **326**, 117609, doi: 10.1016/j.compstruct.2023.117609.
[27] W. Sun, J. O. Jirsa, W. M. Ghannoum, Behavior of anchored carbon fiber-reinforced polymer strips used for strengthening concrete structures, *ACI Materials Journal*, 2016, **113**, 163–172, doi: 10.14359/51688637.
[28] W. Shekarchi, D. Pudleiner, N. Alotaibi, W. Ghannoum, J. Jirsa, Carbon fiber-reinforced polymer spike anchor design recommendations, *ACI Structural Journal*, 2020, **117**, 171–182, doi: 10.14359/51728065.
[29] M. Assad, R. A. Hawileh, J. A. Abdalla, Flexural strengthening of reinforced concrete beams with CFRP laminates and spike anchors, *Composites Part C: Open Access*, 2024, **13**, 100443, doi: 10.1016/j.jcomc.2024.100443.
[30] R. A. Hawileh, M. Assad, J. A. Abdalla, Effect of increasing the number of anchors on the flexural performance of FRP-strengthened RC beams, *Procedia Structural Integrity*, 2024, **54**, 287-293, doi: 10.1016/j.prostr.2024.01.085.
[31] G. S. Alshami, R. A. Hawileh, J. Tatar, J. A. Abdalla, Influence of CFRP spike anchors on the performance of flexural CFRP sheets externally bonded to concrete, *Journal of Composites for Construction*, 2023, **27**, doi: 10.1061/jccof2.cceng-4182.
[32] D. Pudleiner. Design considerations based on size effects of anchored carbon fiber reinforced polymer (CFRP) systems, Doctoral dissertation, The University of Texas at Austin, 2016.
[33] N. K. Alotaibi, W. A. Shekarchi, W. M. Ghannoum, J. O. Jirsa, Shear design of reinforced concrete beams strengthened in shear with anchored carbon fiber-reinforced polymer (CFRP) strips, *ACI Structural Journal*, 2020, **117**, 171–182, doi: 10.14359/51721315.
[34] A. T. Al-Sammari, S. F. Breña, Strength of carbon fiber-reinforced polymer (CFRP) sheets bonded to concrete with CFRP spike anchors, *ACI Structural Journal*, 2021, **118**, 153–166, doi: 10.14359/51728084.
[35] A. Committee, 440.2R-17: Guide for the design and construction of externally bonded frp systems for strengthening concrete structures, American Concrete Institute, 2017.
[36] M. A. Zaki, H. A. Rasheed, T. Alkhrdaji, Performance of CFRP-strengthened concrete beams fastened with distributed CFRP dowel and fiber anchors, *Composites Part B: Engineering*, 2019, **176**, 107117, doi: 10.1016/j.compositesb.2019.107117.
[37] H. A. Rasheed, M. A. Zaki, M. M. Raheem, Effectiveness of fiber anchors in CFRP flexural strengthening of RC girders, *Journal of Composites for Construction*, 2024, **28**, 04024028, doi: 10.1061/jccof2.cceng-4367.
[38] Standard Test Method for Flexural Strength of Concrete (Using Simple Beam with Center-Point Loading), ASTM C293.17, ASTM International, 2017.
[39] J. Zhang, Analysis of variance for functional data, *Monographs on statistics and applied probability*, 2014, **127**, 127.

